Jpn. J. Appl. Phys. Vol. 39 (2000) pp. 3406–3409
Part 1, No. 6A, June 2000

Low Threshold GaInAsP Lasers with Semiconductor/Air Distributed Bragg Reflector Fabricated by Inductively Coupled Plasma Etching

Maiko ARIGA, Yushi SEKIDO, Atsushi SAKAI, Toshihiko BABA, Akihiro MATSUTANI[1], Fumio KOYAMA[1] and Kenichi IGA[1]

Yokohama National University, Division of Electrical and Computer Engineering, 79-5 Tokiwadai, Hodogayaku, Yokohama, 240-8501, Japan
[1] *Tokyo Institute of Technology, Precision and Intelligence Laboratory, 4259 Nagatsuda, Midoriku, Yokohama, 226-8503, Japan*

(Received October 22, 1999; accepted for publication March 14, 2000)

We fabricated GaInAsP/InP short cavity lasers with semiconductor/air distributed Bragg reflectors (DBRs) by inductively coupled plasma etching with pure Cl_2 gas. Nearly vertical sidewalls with low roughness of $\sim$10 nm were achieved, separated by air spaces of three quarter wavelengths. The lowest threshold current normalized by the stripe width was 3.2 mA/μm. From this value, the DBR reflectivity was evaluated to be 85%, which agreed with the theoretical value obtained from a finite-difference time domain (FDTD) simulation. We compared two types of devices with different DBR shapes, and observed that DBR reflectivity was affected more by the tilt of the DBR sidewalls than the sidewall roughness. This result also agreed well with the FDTD theory.

KEYWORDS: semiconductor laser, GaInAsP/InP, distributed Bragg reflector laser, inductively coupled plasma etching, finite difference time domain simulation

1. Introduction

Laser diodes for access networks and local area data links require simple fabrication processes for easy mass production and high performance, as well as the ease of integration with other elements, for example, waveguides, detectors and filters. A short cavity laser with a semiconductor/air distributed Bragg reflector (DBR)[1–6] is suitable for this purpose. It consists of a stripe cavity with a GaInAsP strained quantum well active layer and semiconductor/air DBRs, which are semiconductor vertical walls separated by air spaces. Such a structure can be monolithically formed by anisotropic etching. The large refractive index contrast allows a high reflectivity even with a small number of periods, so that a short cavity is possible, which gives a low threshold current suitable for zero-bias modulation and single longitudinal mode operation.

However, the fabrication of such DBRs, which are made of InP-based materials, is a challenge. So far, dry and wet etching processes have been used. Using Cl_2 reactive ion beam etching (RIBE), vertical sidewalls were easily achieved, but they were rough and nonuniform.[1,2] Wet etching realized smooth sidewalls, but they were severely tilted.[4] In addition, the mechanism of reflectivity degradation was not clear. In this study, we used inductively coupled plasma (ICP) etching to solve this problem. Using this method, fine and smooth etching has been demonstrated in this material system.[7] We fabricated the DBR and evaluated its reflectivity based on its lasing characteristics. We compared the evaluated reflectivity with the calculated reflectivities obtained using the two-dimensional finite difference time domain (FDTD) method, and investigated the dominant factor required for a high DBR reflectivity.

2. Fabrication of DBR

We prepared an epitaxial wafer grown on n-InP substrate by metal organic vapor phase epitaxy. Epilayers consisted of an n-InP cladding layer, 0.25-μm-thick GaInAsP active layer, 1.7-μm p-InP cladding layer and 0.3-μm p-GaInAs contact layer from the bottom. The active layer consisted of eight compressively-strained quantum-wells of $\sim$4 nm thickness each with 10-nm-thick strain-compensated barriers and gradient-index separate confinement heterostructure layers. The peak wavelength of the spontaneous emission was 1.53 μm, and the lasing wavelength of the broad area lasers was typically 1.55 μm. The design and the fabrication process were similar to that reported previously[1,2] except for the etching method. The width of the stripe w was 20 μm. The cavity length L, i.e., length of the stripe, was varied from 150 to 250 μm in the samples. The DBR was placed at one end of the stripe as a backside mirror, and for the other end, a simple etched facet was used as a front mirror. The width of the DBR was designed to be twice the stripe width, i.e., 40 μm, to avoid the influence of fragile side edges of the DBR. The thicknesses of the semiconductor walls and air spaces were three quarters the lasing wavelength λ in the media, i.e., 0.35 μm and 1.15 μm, respectively, for $\lambda = 1.55\,\mu$m. The number of semiconductor/air pairs N was fixed at 4. According to the FDTD calculation of the DBR reflectivity, $N = 3$ is sufficient to obtain the maximum reflectivity limited by the diffraction loss in air spaces. However, a larger N was effective for reducing the nonuniformity of the thickness of the semiconductor walls.

During the fabrication process, AuZn and AuGe electrodes were formed on the epitaxial and back surfaces of the wafer, respectively. After patterning the AuZn electrode into a rectangular shape, the DBR pattern was drawn on this side by electron beam lithography using negative resist SAL601-SR7 (Shipley Co., Inc.), and the epilayers were etched using the ICP etching machine RIE-101ip (SAMCO International Inc.) with pure Cl_2 gas. The gas flow rate was 10.0 sccm and the gas pressure was 0.5 Pa. The ICP power and the bias power were 300 W and 200 W, respectively. Under these conditions, the etch rate of InP was nearly 1.0 μm/min. Figure 1 shows the scanning electron micrograph (SEM) of the sample. The sidewall angle was more than 89° and the sidewall roughness estimated roughly was less than 10 nm.

3. Lasing Characteristics

For measurement purposes, the wafers were cut into pieces, as each of them had one device chip. Each piece was placed n-side down on a submount without a metal bonding. Figure 2 shows typical lasing characteristics of a sample of cav-

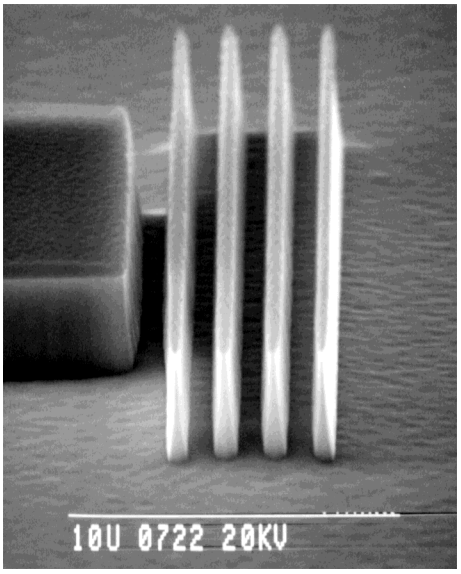

Fig. 1. Side view of fabricated DBR.

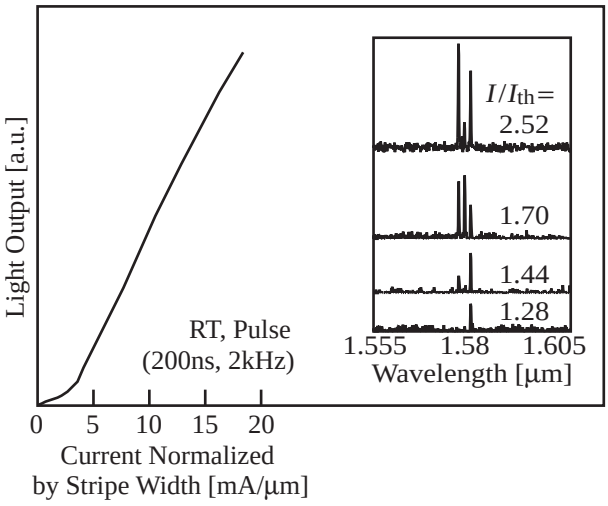

Fig. 2. Light output versus normalized current characteristics and lasing spectra measured for a device with cavity length of 250 μm.

ity length $L = 250\,\mu$m at room temperature under the pulsed condition (pulse width of 200 ns and repetition frequency of 2 kHz). In Fig. 2, the current is normalized by the stripe width w. The lowest normalized threshold current I_{th}/w was 3.2 mA/μm. This value is nearly the same as that recorded for an $L = 100\,\mu$m device fabricated by RIBE etching.[2)] The spectra show multimode lasing characteristics, as shown in the inset of Fig. 2. This is due to the wide stopband of this type of DBR. The single mode operation can be obtained by reducing the cavity length to less than 50 μm.

We observed a clear relationship between the DBR shapes and the etched facet at the other end, and the lasing characteristics. Using the different chamber conditions, we obtained two types of devices with different shapes of DBR. The lasing characteristics of these devices and SEM photographs are summarized in Fig. 3. Device A had an nearly vertical semiconductor sidewalls with relatively high roughness of over 20 nm. Device B had tapered sidewalls with low roughness of ~10 nm. The shapes and roughnesses of the etched facets in these devices were almost the same as those of the DBR. It

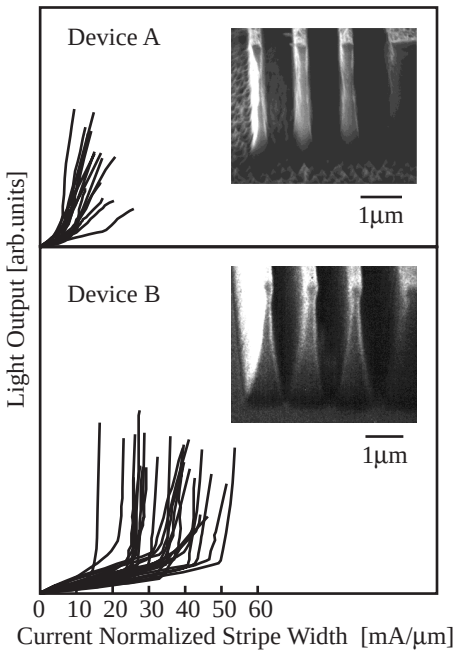

Fig. 3. Side views and lasing characteristics of two types of devices A and B.

is clear that the threshold current was much lower for device A than device B.

In Fig. 4, we plot the measured threshold current density J_{th} with the inverse cavity length L^{-1}. Straight lines indicate theoretical values obtained by assuming the logarithmic gain $g = g_0 \ln(J/J_0)$ for strained quantum-wells, and the current density for transparency $J_0 = 512\,\mathrm{A/cm^2}$, a gain coefficient $g_0 = 627\,\mathrm{cm^{-1}}$ and an internal cavity loss of $5\,\mathrm{cm^{-1}}$, which were evaluated for cleaved lasers. Experimental data for cavity lengths show relatively large dispersion values. This is mainly due to the irregular scattering loss at stripe mesas, etched facets and DBRs, which are mechanically damaged due to the cleaving of the wafer and mounting of each device chip on a submount with a metal fitting. We estimated the

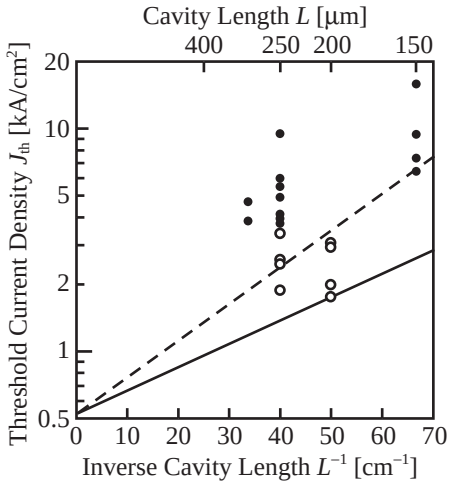

Fig. 4. Threshold current density versus inverse cavity length characteristics. Open and closed circles indicate devices A and B, respectively. Solid line indicates theoretical results obtained by assuming DBR reflectivity R_{DBR} of 85% and facet reflectivity R_f of 28%. The dashed lines indicate results when $R_{DBR} = 50\%$ and $R_f = 10\%$ are assumed.

reflectivity of the etched facet and the DBR by fitting a theoretical curve with the minimum threshold current density for each type of device. We fabricated simple stripe lasers without DBRs but with a set of etched facets, along with DBR lasers. We first evaluated the reflectivity of the etched facet by measuring J_{th} for these lasers. It was 28% and 10% for devices A and B, respectively. Based on these results, the DBR reflectivity of device A, which recorded the lowest J_{th}, was evaluated to be 85%. On the other hand, the reflectivity was 50% for device B. Differences in the facet and DBR reflectivities indicate that the reflectivity is strongly affected by the tilt of the semiconductor sidewalls and is not very sensitive to the sidewall roughness.

4. Considerations

We compared the obtained reflectivities with those calculated by the FDTD method.[8] For the calculation, we used Yee's 20-nm-square cells, dividing the model of the laser structure viewed from the lateral direction, as shown in Fig. 5. We assumed an infinite lateral width and a transverse electric field of the laser mode. A Gaussian pulse of 40 fs full width at $1/e^2$ maximum with the guided mode profile in the laser waveguide was used as an excitation field. The DBR reflectivity was evaluated by calculating the overlap integral between the profile of the analytical guided mode in the waveguide and that of the light pulse reflected by the DBR and coupled again to the waveguide. We input the measured data of the DBR shapes of devices A and B into a computer. Figure 6 shows the reflection spectra of the DBRs, which were obtained by the Fourier transform of the time series of the overlap integral. For these devices, the stopband lies within 1.3 μm to 1.7 μm. The peak reflectivity is at a shorter wavelength than the stopband center, since the longer wavelength light suffers a larger diffraction loss in air spaces. Experimental values indicated by open circles nearly agree with the calculated ones.

As discussed in the previous section, the sidewall angle of the semiconductor is more crucial for the DBR reflectivity than the sidewall roughness. We calculated the angle dependence of the reflectivity at $\lambda = 1.55\,\mu$m and at the wavelength giving the peak reflectivity, as shown in Fig. 7. The reflectivity is strongly affected by the tilt of the sidewall; a tilt of only 5° reduces the reflectivity to ~30%.

We also investigated the behavior of light around the DBR in device A by the FDTD method. The light pulse reflected by the DBR is displayed in Fig. 8. From this figure, we es-

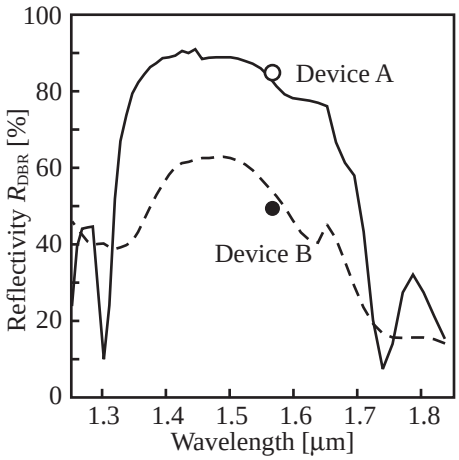

Fig. 6. Reflection spectra of DBRs. Solid and dashed curves indicate theoretical values for devices A and B, respectively. Open and closed circles indicate experimental values for these devices.

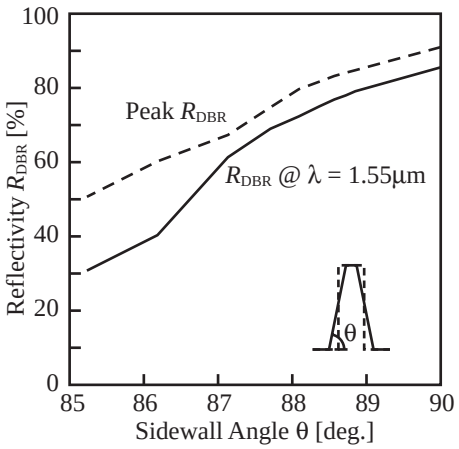

Fig. 7. DBR reflectivity calculated with sidewall angle.

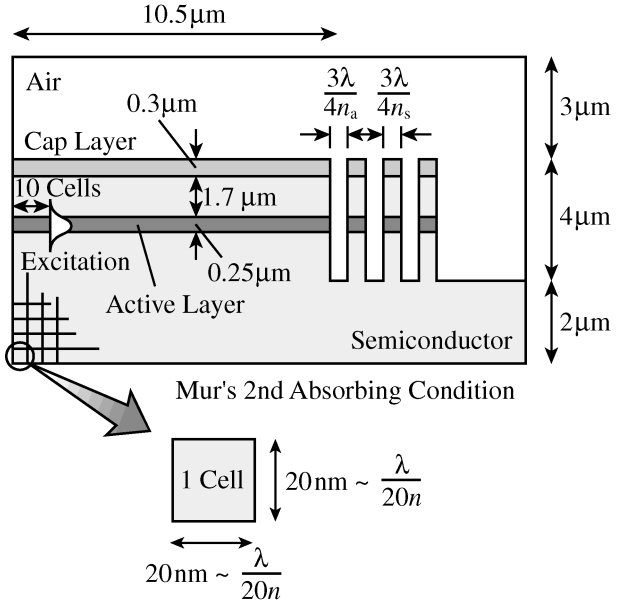

Fig. 5. FDTD calculation model.

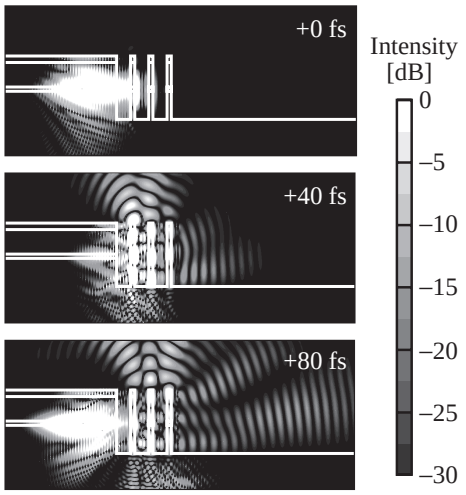

Fig. 8. Intensity profiles around DBR in device A.

timated the amount of light power scattered in each direction by the DBR. 85% light power was reflected and coupled to the waveguide, as mentioned above, and 9.2% was reflected but not coupled to the waveguide. This causes a decrease in the external quantum efficiency. In addition, 3.5% is deflected upward, 2.0% is deflected downward, and 0.3% passes through the DBR to the right. Therefore, even if we install a monitor detector on the right hand side of such a DBR, it will still be difficult to obtain high efficiency. We have reported that the diffraction loss can be significantly reduced by narrowing the air space to $\lambda/4$, i.e., $0.39\,\mu$m for $\lambda = 1.55\,\mu$m.[9] However, this narrow space is difficult to fabricate without severe optimization of etching conditions. We also determined that, even though the air spaces are designed to be $3\lambda/4$, the diffraction loss in the spaces can be suppressed and the maximum reflectivity can be improved to $>90\%$ by plugging the spaces with some transparent material such as a polyimide with a refractive index of $\sim$1.6. High-performance lasing has been demonstrated by plugging the spaces with benzocyclobutene (BCB) polymer.[6]

5. Conclusions

We fabricated a high reflectivity semiconductor/air DBR by ICP etching with pure Cl_2 gas. The DBR had smooth sidewalls with an angle of more than 89° against the substrate plane and roughness of less than 10 nm. In a GaInAsP/InP stripe laser system with such a DBR at one end, the minimum threshold current normalized by the stripe width was as low as $3.2\,\text{mA}/\mu$m. The evaluated reflectivity was 85%, which agreed well with the theoretical value obtained by the FDTD method. We experimentally and theoretically confirmed that the tilt of the vertical sidewall was more crucial for obtaining a high-reflectivity DBR than the roughness of the sidewall.

Acknowledgments

We would like to thank Professor Y. Kokubun, Professor Y. Hirose and Associate Professor H. Arai, Yokohama National University, for their valuable discussions.

1) T. Baba, M. Hamasaki, N. Watanabe, P. Kaeplung, A. Matsutani, T. Mukaihara, F. Koyama and K. Iga: Jpn. J. Appl. Phys. **35** (1996) 1390.
2) M. Hamasaki, P. Kaewplung, T. Baba, A. Matsutani, F. Koyama and K. Iga: Proc. Optelectronic and Communication Conf., Makuhari (1996) 18P-31.
3) Y. Yuan, T. Brock, P. Bhattacharya, C. Caneau and R. Bhat: IEEE Photon. Technol. Lett. **9** (1997) 881.
4) T. Mukaihara, N. Yamanaka, N. Iwai, T. Ishikawa and A. Kasukawa: Electron. Lett. **34** (1998) 882.
5) E. Höfling, R. Werner, F. Schäfer, J. P. Reithmaier and A. Forchel: Electron. Lett. **35** (1999) 154.
6) M. M. Raj, Y. Saka, J. Wiedmann, H. Yasumoto and S. Arai: Jpn. J. Appl. Phys. **38** (1999) L1240.
7) A. Matsutani, H. Ohtsuki, F. Koyama and K. Iga: Jpn. J. Appl. Phys. **38** (1999) 4260.
8) R. Jambunathan and J. Singh: IEEE J. Quantum Electron. **33** (1997) 1180.
9) N. Habu, H. Tago, T. Baba, A. Matsutani, F. Koyama and K. Iga: Ext. Abstr. Fall Meet. Japan Society of Applied Physics, 1996, 8p-KH-16 [in Japanese].